International Journal of Bifurcation and Chaos, Vol. 25, No. 6 (2015) 1550085 (13 pages)
© World Scientific Publishing Company
DOI: 10.1142/S0218127415500856

Characteristic Analysis and DSP Realization of Fractional-Order Simplified Lorenz System Based on Adomian Decomposition Method

Huihai Wang, Kehui Sun* and Shaobo He
School of Physics and Electronics,
Central South University, Changsha,
Hunan 410083, P. R. China

**School of Physics Science and Technology,*
Xinjiang University, Urumqi,
Xinjiang 830046, P. R. China
**kehui@csu.edu.cn*

Received July 30, 2014; Revised November 30, 2014

By adopting Adomian decomposition method, the fractional-order simplified Lorenz system is solved and implemented on a digital signal processor (DSP). The Lyapunov exponent (LE) spectra of the system is calculated based on QR-factorization, and it accords well with the corresponding bifurcation diagrams. We analyze the influence of the parameter and the fractional derivative order on the system characteristics by color maximum LE (LE_{max}) and chaos diagrams. It is found that the smaller the order is, the larger the LE_{max} is. The iteration step size also affects the lowest order at which the chaos exists. Further, we implement the fractional-order simplified Lorenz system on a DSP platform. The phase portraits generated on DSP are consistent with the results that were obtained by computer simulations. It lays a good foundation for applications of the fractional-order chaotic systems.

Keywords: Fractional calculus; simplified Lorenz system; Adomian decomposition method; Lyapunov exponent diagram; digital signal processor.

1. Introduction

Numerical solution method is one of the critical problems in theoretical research and in the applications of fractional-order chaotic systems. At present, three methods were mainly used in the previous literature: frequency domain approximation [Sun *et al.*, 1984], predictor-corrector method (PCM) [Diethelm, 1997], and Adomian decomposition method (ADM) [Adomian, 1984]. The step size of order for frequency domain approximation is too large, and its precision is limited. Whether this method accurately reflects the chaos characteristics of a fractional-order nonlinear system was questioned in some literature [Tavazoei & Haeri, 2007, 2008]. For PCM, one can obtain more accurate results, and it is used to analyze the dynamical characteristics of a fractional-order system when the order changes continuously. But the calculation speed is very slow, and it consumes too much computer resources. Thus, it is unsuitable for engineering practice. Compared with the two solution approaches, ADM is capable of dealing with linear and nonlinear problems in time domain [Cafagna & Grassi, 2008, 2009]. He *et al.* [2014] concluded the

*Author for correspondence

characteristics of this method, such as high accuracy, fast convergence and less computer resources consumption, so ADM becomes one of the best candidate methods for solving fractional-order chaotic system at present.

The Lyapunov exponent (LE) spectrum is one of the effective methods in researching dynamical characteristics of nonlinear systems, but calculating the LE spectrum of a fractional-order chaotic system is a challenging problem. Caponetto and Fazzino [2013] employed ADM to simulate and analyze fractional-order chaotic systems, but it only calculated its LE spectra with several different orders. In fact, maximum LE ($\mathrm{LE}_{\max}$) diagram [Stegemann *et al.*, 2011; Xavier & Rech, 2010] and chaos diagram [Salau & Ajide, 2012; Tao & Ue, 2014] are better choices for analyzing the dynamical behaviors of chaotic systems by varying two parameters simultaneously. In [Sun *et al.*, 2010a], the dynamical characteristics of the fractional-order simplified Lorenz system were analyzed by adopting PCM. For comparison, we solve and analyze the same system by adopting ADM.

Fractional-order chaotic system applications have been investigated in many fields, such as nuclear magnetic resonance [Bhalekar *et al.*, 2012], cellular neural network [Çelik & Demir, 2010] and secure communication [Kiani-B *et al.*, 2009], and some good results were obtained. Their realizations depend on the software and hardware technologies of signal processing. Digital signal processor (DSP) is popularized in engineering because of its performance and convenience in signal processing. So DSP implementations of fractional-order chaotic systems are very useful for their applications. To our knowledge, fractional-order differentiators and integrators were experimented on DSP by using frequency domain approximation [Krishna, 2011], and integer-order chaotic systems were realized and applied on DSP in many fields [Rhouma & Belghith, 2011; Hermassi *et al.*, 2013]. However, DSP implementations of fractional-order chaotic systems were rarely reported.

In this paper, we focus on solving and analyzing the fractional-order simplified Lorenz system by adopting ADM and its implementation on DSP. The paper is organized as follows. In Sec. 2, ADM is introduced briefly, and the iterative algorithm of the fractional-order simplified Lorenz system is presented. In Sec. 3, the dynamical characteristics of this system are analyzed by LE spectra, bifurcation diagrams and 0–1 test. Also, the color $\mathrm{LE}_{\max}$ diagram and chaos diagram are constructed. In Sec. 4, the fractional-order chaotic system is realized on DSP. Finally, we summarize the results and indicate future directions.

2. Numerical Solution of Fractional-Order Simplified Lorenz System

2.1. *Adomian decomposition method*

For a given fractional-order differential equation

$$ {}^{*}D_{t_0}^{q}\mathbf{x}(t) = f(\mathbf{x}(t)), $$

here $\mathbf{x}(t) = [x_1(t), x_2(t), \ldots, x_n(t)]^T$ are variables, and ${}^{*}D_{t_0}^{q}$ is the Caputo derivative operator of order $q(m-1 < q \le m, m \in N)$ [Gorenflo & Mainardi, 1997]. To obtain the following initial value problem, $f(\mathbf{x}(t))$ is separated into three terms [Momani & Al-Khaled, 2005; Daftardar-Gejji & Jafari, 2005],

$$ \begin{cases} {}^{*}D_{t_0}^{q}\mathbf{x}(t) = L\mathbf{x}(t) + N\mathbf{x}(t) + \mathbf{g}(t) \\ \mathbf{x}^{(k)}(t_0^{+}) = \mathbf{b}_k, \quad k = 0, \ldots, m-1. \end{cases} \tag{1} $$

Here, L and N represent linear and nonlinear operators, respectively, and $\mathbf{g}(t) = [g_1(t), g_2(t), \ldots, g_n(t)]^T$ are constants for autonomous systems, and $\mathbf{b}_k$ is a specified constant. By applying the operator $J_{t_0}^{q}$ to both sides of Eq. (1), the following equation is obtained [Shawagfeh, 2002]:

$$ \mathbf{x} = J_{t_0}^{q}L\mathbf{x} + J_{t_0}^{q}N\mathbf{x} + J_{t_0}^{q}\mathbf{g} + \sum_{k=0}^{m-1}\mathbf{b}_k\frac{(t-t_0)^k}{k!}. \tag{2} $$

$J_{t_0}^{q}$ is Riemann–Liouville fractional integral operator of order q. For $t \in [t_0, t_1]$, $q \ge 0$, $r \ge 0$, $\gamma > -1$ and real constant C, the fundamental properties of the integral operator $J_{t_0}^{q}$ are described as follows [Gorenflo & Mainardi, 1997]:

$$ J_{t_0}^{q}(t-t_0)^{\gamma} = \frac{\Gamma(\gamma+1)}{\Gamma(\gamma+1+q)}(t-t_0)^{\gamma+q}, \tag{3} $$

$$ J_{t_0}^{q}C = \frac{C}{\Gamma(q+1)}(t-t_0)^{q}, \tag{4} $$

$$ J_{t_0}^{q}J_{t_0}^{r}x(t) = J_{t_0}^{q+r}x(t). \tag{5} $$

Based on ADM, the nonlinear terms of Eq. (2) are decomposed according to

$$\begin{cases} A_j^i = \dfrac{1}{i!}\left[\dfrac{d^i}{d\lambda^i}N(\nu_j^i(\lambda))\right]_{\lambda=0} \\ \nu_j^i(\lambda) = \displaystyle\sum_{k=0}^{i}(\lambda)^k x_j^k, \end{cases} \tag{6}$$

where $i = 0, 1, \ldots, \infty$; $j = 1, \ldots, n$. Then the nonlinear terms are expressed as

$$N\mathbf{x} = \sum_{i=0}^{\infty}\mathbf{A}^i(\mathbf{x}^0, \mathbf{x}^1, \ldots, \mathbf{x}^i). \tag{7}$$

So the solution of Eq. (1), $\mathbf{x} = \sum_{i=0}^{\infty}\mathbf{x}^i$ is derived from

$$\begin{cases} \mathbf{x}^0 = J_{t_0}^q\mathbf{g} + \displaystyle\sum_{k=0}^{m-1}\mathbf{b}_k\frac{(t-t_0)^k}{k!} \\ \mathbf{x}^1 = J_{t_0}^q L\mathbf{x}^0 + J_{t_0}^q\mathbf{A}^0(\mathbf{x}^0) \\ \mathbf{x}^2 = J_{t_0}^q L\mathbf{x}^1 + J_{t_0}^q\mathbf{A}^1(\mathbf{x}^0, \mathbf{x}^1) \\ \quad\vdots \\ \mathbf{x}^i = J_{t_0}^q L\mathbf{x}^{i-1} + J_{t_0}^q\mathbf{A}^{i-1}(\mathbf{x}^0, \mathbf{x}^1, \ldots, \mathbf{x}^{i-1}) \\ \quad\vdots \end{cases}. \tag{8}$$

2.2. *Solution of the fractional-order simplified Lorenz system*

The equation of the fractional-order simplified Lorenz system is

$$\begin{cases} {}^*D_{t_0}^q x = 10(y-x) \\ {}^*D_{t_0}^q y = (24-4c)x - xz + cy \\ {}^*D_{t_0}^q z = xy - \dfrac{8}{3}z, \end{cases} \tag{9}$$

where x, y, z are the state variables, and $q(0 < q \leq 1)$ is the order of fractional-order differential equation, and c is the system parameter. According to Eqs. (3)–(5) and (8), the discrete iterative formula of the system (9) is presented by

$$\begin{cases} x_{m+1} = x_m + 10(y_m - x_m)\dfrac{h^q}{\Gamma(q+1)} + 10[(24-4c)x_m + cy_m - 10(y_m - x_m)]\dfrac{h^{2q}}{\Gamma(2q+1)} + \cdots \\ y_{m+1} = y_m + [(24-4c)x_m + cy_m - x_m z_m]\dfrac{h^q}{\Gamma(q+1)} \\ \qquad + \{10(24-4c)(y_m - x_m) + c[(24-4c)x_m + cy_m - x_m z_m] + \cdots\}\dfrac{h^{2q}}{\Gamma(2q+1)} + \cdots \\ z_{m+1} = z_m + \left(x_m y_m - \dfrac{8}{3}z_m\right)\dfrac{h^q}{\Gamma(q+1)} + \left\{-\dfrac{8}{3}\left[-\dfrac{8}{3}z_m + x_m y_m\right] + 10y_m(y_m - x_m) + \cdots\right\} \\ \qquad \times \dfrac{h^{2q}}{\Gamma(2q+1)} + \cdots, \end{cases} \tag{10}$$

where h is iteration step size. $\Gamma(\cdot)$ is Gamma function. Considering the fast convergence of this method [Abbaoui & Cherruault, 1994], we truncate the first seven terms of Eq. (10) in this paper. For the computer simulation and DSP implementation, the iteration is expressed as Eqs. (11)–(18).

$$\begin{cases} C_{10} = x_m \\ C_{20} = y_m \\ C_{30} = z_m, \end{cases} \tag{11}$$

$$\begin{cases} C_{11} = 10(C_{20} - C_{10}) \\ C_{21} = (24 - 4c)C_{10} + cC_{20} - C_{10}C_{30} \\ C_{31} = -\dfrac{8}{3}C_{30} + C_{10}C_{20}, \end{cases} \tag{12}$$

$$\begin{cases} C_{12} = 10(C_{21} - C_{11}) \\ C_{22} = (24 - 4c)C_{11} + cC_{21} - C_{11}C_{30} - C_{10}C_{31} \\ C_{32} = -\dfrac{8}{3}C_{31} + C_{11}C_{20} + C_{10}C_{21}, \end{cases} \tag{13}$$

$$\begin{cases} C_{13} = 10(C_{22} - C_{12}) \\ C_{23} = (24 - 4c)C_{12} + cC_{22} - C_{12}C_{30} - C_{11}C_{31}\dfrac{\Gamma(2q+1)}{\Gamma^2(q+1)} - C_{10}C_{32} \\ C_{33} = -\dfrac{8}{3}C_{32} + C_{12}C_{20} + C_{11}C_{21}\dfrac{\Gamma(2q+1)}{\Gamma^2(q+1)} + C_{10}C_{22}, \end{cases} \tag{14}$$

$$\begin{cases} C_{14} = 10(C_{23} - C_{13}) \\ C_{24} = (24 - 4c)C_{13} + cC_{23} - C_{13}C_{30} - (C_{12}C_{31} + C_{11}C_{32}) \\ \qquad \times \dfrac{\Gamma(3q+1)}{\Gamma(q+1)\Gamma(2q+1)} - C_{10}C_{33} \\ C_{34} = -\dfrac{8}{3}C_{33} + C_{13}C_{20} + (C_{12}C_{21} + C_{11}C_{22})\dfrac{\Gamma(3q+1)}{\Gamma(q+1)\Gamma(2q+1)} + C_{10}C_{23}, \end{cases} \tag{15}$$

$$\begin{cases} C_{15} = 10(C_{24} - C_{14}) \\ C_{25} = (24 - 4c)C_{14} + cC_{24} - C_{14}C_{30} - (C_{13}C_{31} + C_{11}C_{33})\dfrac{\Gamma(4q+1)}{\Gamma(q+1)\Gamma(3q+1)} \\ \qquad - C_{12}C_{32}\dfrac{\Gamma(4q+1)}{\Gamma^2(2q+1)} - C_{10}C_{34} \\ C_{35} = -\dfrac{8}{3}C_{34} + C_{14}C_{20} + (C_{13}C_{21} + C_{11}C_{23})\dfrac{\Gamma(4q+1)}{\Gamma(q+1)\Gamma(3q+1)} \\ \qquad + C_{12}C_{22}\dfrac{\Gamma(4q+1)}{\Gamma^2(2q+1)} + C_{10}C_{24}, \end{cases} \tag{16}$$

$$\begin{cases} C_{16} = 10(C_{25} - C_{15}) \\ C_{26} = (24-4c)C_{15} + cC_{25} - C_{15}C_{30} - (C_{14}C_{31} + C_{11}C_{34})\dfrac{\Gamma(5q+1)}{\Gamma(q+1)\Gamma(4q+1)} \\ \qquad - (C_{13}C_{32} + C_{12}C_{33})\dfrac{\Gamma(5q+1)}{\Gamma(2q+1)\Gamma(3q+1)} - C_{10}C_{35} \\ C_{36} = -\dfrac{8}{3}C_{35} + C_{15}C_{20} + (C_{14}C_{21} + C_{11}C_{24})\dfrac{\Gamma(5q+1)}{\Gamma(q+1)\Gamma(4q+1)} \\ \qquad + (C_{13}C_{22} + C_{12}C_{23})\dfrac{\Gamma(5q+1)}{\Gamma(2q+1)\Gamma(3q+1)} + C_{10}C_{25}, \end{cases} \tag{17}$$

$$\begin{bmatrix} x_{m+1} \\ y_{m+1} \\ z_{m+1} \end{bmatrix} = \begin{bmatrix} C_{10} & C_{11} & C_{12} & C_{13} & C_{14} & C_{15} & C_{16} \\ C_{20} & C_{21} & C_{22} & C_{23} & C_{24} & C_{25} & C_{26} \\ C_{30} & C_{31} & C_{32} & C_{33} & C_{34} & C_{35} & C_{36} \end{bmatrix}$$

$$\times \begin{bmatrix} 1 & \dfrac{h^q}{\Gamma(q+1)} & \dfrac{h^{2q}}{\Gamma(2q+1)} & \dfrac{h^{3q}}{\Gamma(3q+1)} & \dfrac{h^{4q}}{\Gamma(4q+1)} & \dfrac{h^{5q}}{\Gamma(5q+1)} & \dfrac{h^{6q}}{\Gamma(6q+1)} \end{bmatrix}^T. \tag{18}$$

According to Eqs. (11)–(18), the chaotic sequences of the fractional-order simplified Lorenz system are obtained with initial values, h, q and appropriate parameters. Then we can analyze the dynamical characteristics of the system by using the chaotic sequences.

3. Analysis of Dynamical Characteristics

3.1. *Lyapunov exponent spectra*

Based on the iteration formula, we design the LE spectra calculation algorithm of the fractional-order chaotic system by employing QR-factorization. In this algorithm, QR-factorization is described as [Von Bremen *et al.*, 1997]

$$\begin{aligned} & qr[\mathbf{J}_m\mathbf{J}_{m-1}\cdots\mathbf{J}_1] \\ &= qr[\mathbf{J}_m\mathbf{J}_{m-1}\cdots\mathbf{J}_2(\mathbf{J}_1\mathbf{Q}_0)] \\ &= qr[\mathbf{J}_m\mathbf{J}_{m-1}\cdots\mathbf{J}_3(\mathbf{J}_2\mathbf{Q}_1)][\mathbf{R}_1] \\ &= \cdots \\ &= qr[\mathbf{J}_m\mathbf{J}_{m-1}\cdots(\mathbf{J}_i\mathbf{Q}_{i-1})][\mathbf{R}_{i-1}\mathbf{R}_{i-2}\cdots\mathbf{R}_2\mathbf{R}_1] \\ &= \cdots \\ &= \mathbf{Q}_m[\mathbf{R}_m\cdots\mathbf{R}_2\mathbf{R}_1] \\ &= \mathbf{Q}_m\mathbf{R}. \end{aligned} \tag{19}$$

Here, $qr[\cdot]$ denotes the QR-factorization process. $\mathbf{J}$ is Jacobian matrix, and the subscript m represents the number of iterations. Then we obtain LE spectra by

$$\lambda_k = \frac{1}{mh}\sum_{i=1}^{m}\ln|\mathbf{R}_i(k,k)|, \tag{20}$$

where k is the system dimension.

Setting $h = 0.01$, Fig. 1 shows the LE spectra and bifurcation diagrams of system (9) based on Eqs. (19) and (20). In the case of $q = 0.9$ and c varying, the system enters into chaotic state at $c = -1.1$ as shown in Fig. 1(a). The $\mathrm{LE}_{\max}$ gradually decreases as the increases of c, and the system enters into the quasiperiodic state at $c = 7.2$. It is consistent with the corresponding bifurcation diagram as shown in Fig. 1(b). Similarly, Figs. 1(c) and 1(d) are in good agreement, too. In the case of $c = 5$ and q varying, the system enters into chaotic state at $q = 0.595$. Although the $\mathrm{LE}_{\max}$ also gradually decreases with the increase of q, it is chaotic except for a small periodic window at $q = 0.88$. So, the LE spectra calculation algorithm is reliable.

Keeping $h = 0.01$, we plot the $\mathrm{LE}_{\max}$ for different q versus c as shown in Fig. 2. For any q, with the increase of c, the $\mathrm{LE}_{\max}$ decreases gradually to zero, and at last becomes negative. Namely, the system becomes convergent from chaotic through periodic.

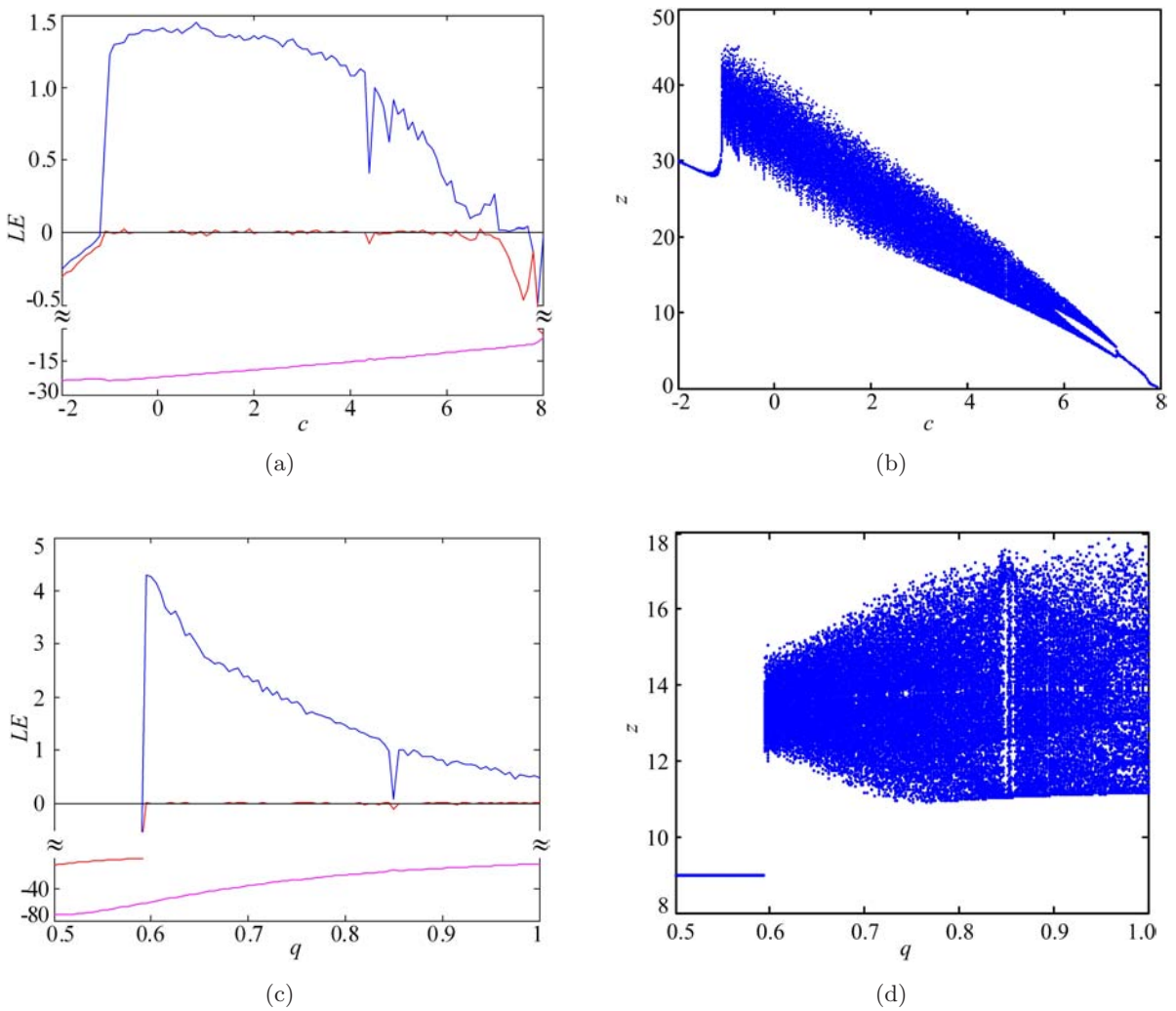

Fig. 1. Lyapunov exponent spectra and bifurcation diagrams for the fractional-order simplified Lorenz system: (a) Lyapunov exponent spectrum, $q = 0.9$; (b) bifurcation diagram, $q = 0.9$; (c) Lyapunov exponent spectrum, $c = 5$ and (d) bifurcation diagram, $c = 5$.

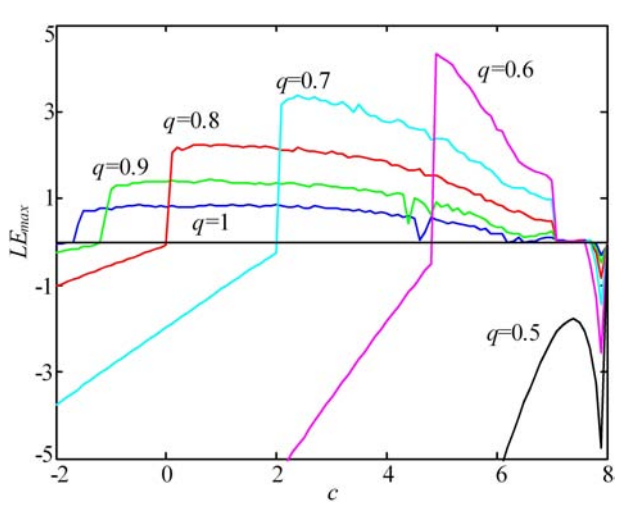

Fig. 2. Maximum Lyapunov exponent with different q versus parameter c.

In addition, the larger q is, the wider is the chaos range. For parameter c, when the system is chaotic, the smaller q is, the larger the $\mathrm{LE}_{\max}$ is. The magnitude of $\mathrm{LE}_{\max}$ also indicates the complexity of a chaotic system. So we come to the conclusion that the fractional-order simplified Lorenz system is more complex than its integer-order counterpart, and it indicates that the fractional-order chaotic system has broader applications.

3.2. *Maximum Lyapunov exponent diagram and chaos diagram*

According to the LE spectra calculation algorithm, we let $h = 0.01$, and the $\mathrm{LE}_{\max}$ diagram of the fractional-order simplified Lorenz system by

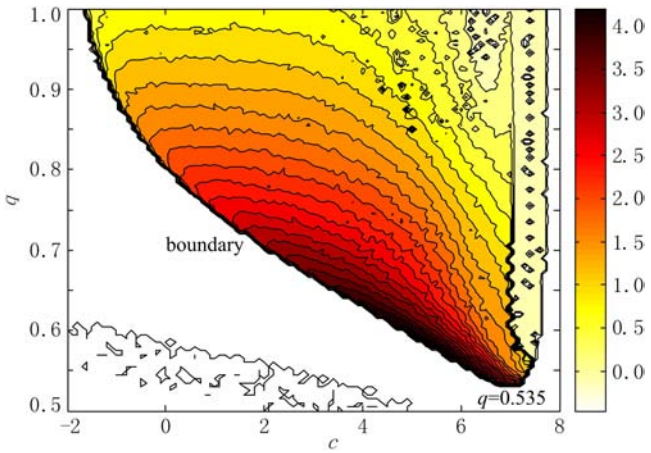

Fig. 3. Maximum Lyapunov exponent diagram for the fractional-order simplified Lorenz system.

changing q and c simultaneously as shown in Fig. 3. It indicates the magnitude of $\mathrm{LE}_{\max}$ for system (9) versus $c \in [-2, 8]$ with the step size of 0.1 and $q \in [0.5, 1]$ with the step size of 0.005. The $\mathrm{LE}_{\max}$ diagram can help us to choose the parameters if a more complex chaotic system is needed in the practical application. In Fig. 3, when $c = 5.3$ and $q = 0.585$, the largest $\mathrm{LE}_{\max}$ is 4.443. It is worthwhile to note that there is a boundary where $\mathrm{LE}_{\max}$ changes suddenly in Fig. 3. On the upside of the boundary along the direction of both q and c increasing, $\mathrm{LE}_{\max}$ decreases gradually, and tends to zero finally. In the opposite direction, $\mathrm{LE}_{\max}$ becomes negative quickly. Namely, the system immediately becomes convergent from chaotic in this direction. To choose larger $\mathrm{LE}_{\max}$, the parameters which are near upper part of the boundary should be selected. The parameters just on the boundary should be avoided, because the system becomes convergent easily for any small unstable factors. In addition, in Fig. 3, the lowest order at which the chaos exists is 3 (the dimension of the system) $\times\, q = 1.605$ when $c \in [6.7, 7.2]$ and $q = 0.535$.

To show the state of the fractional-order chaotic system with different q and c more clearly, in particular period state, the chaos diagram is also plotted on the basis of the magnitude of $\mathrm{LE}_{\max}$. Considering the influence of calculation error and data interception, it has been verified by experiments that the system becomes approximate periodically when $\mathrm{LE}_{\max} = 0.03$. So we determine that the system (9) is chaotic when $\mathrm{LE}_{\max} > 0.03$, and periodic when $0 \le \mathrm{LE}_{\max} \le 0.03$, and convergent when $\mathrm{LE}_{\max} < 0$. The chaos diagram is presented in Fig. 4. Red, blue, black and white represent chaotic, periodic, convergent and emanative, respectively. It is obvious that most regions are chaotic in Fig. 4. The system is convergent for most of q except a small part of periodic when c is small. It indicates that the system enters into chaotic state through periodic when c is small and q is large. It is consistent with that shown in Fig. 2. The chaotic region becomes larger with the increase of c. Periodic region begins to appear partly when $c \in [6.1, 7.7]$. The system becomes convergent when c is larger.

3.3. *0–1 test*

To confirm the lowest order of system (9), we implement the 0–1 test method. 0–1 test is a novel test approach to determine whether a given deterministic nonlinear dynamic system is chaotic. It was proposed by Gottwald and Melbourne [2004], and has already been successfully tested for integer-order chaotic systems [Sun *et al.*, 2010b] and fractional-order chaotic systems [Cafagna & Grassi, 2010; Xin & Li, 2013]. For a fractional-order system, if a set of discrete data $\phi(n)$ $(n = 1, 2, 3, \ldots)$ represents a one-dimensional observable data set obtained from the iterative, then the following two real-valued functions are defined [Cafagna & Grassi, 2008]:

$$\begin{cases} p(n) = \displaystyle\sum_{j=1}^{n} \phi(j)\cos(\theta(j)) \\ s(n) = \displaystyle\sum_{j=1}^{n} \phi(j)\sin(\theta(j)), \end{cases} \tag{21}$$

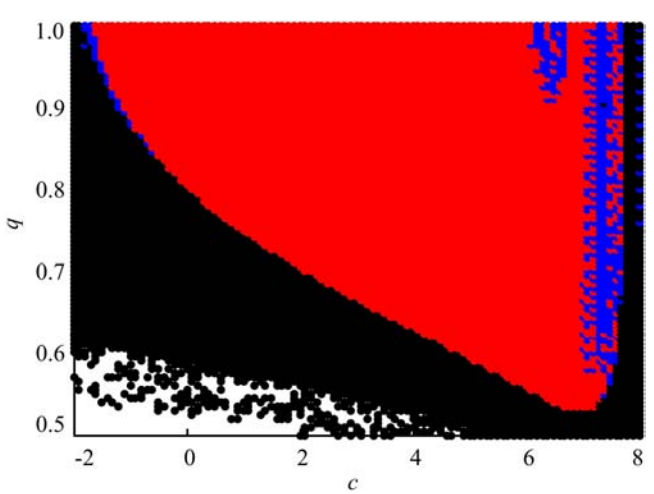

Fig. 4. Chaos diagram for the fractional-order simplified Lorenz system.

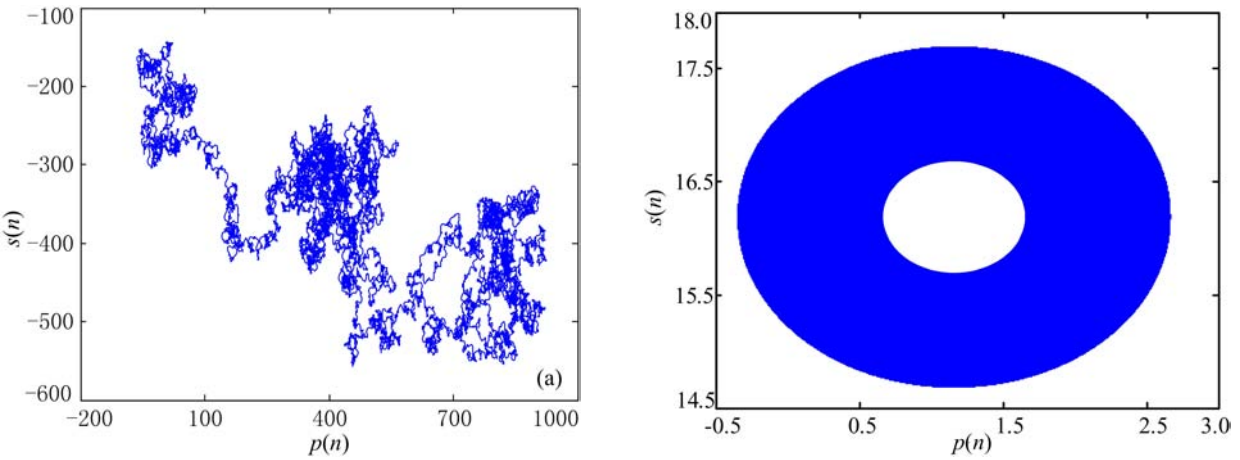

(a) (b)

Fig. 5. For $h = 0.01$ and $c = 7$, the (p, s)-plane for the fractional-order simplified Lorenz system, (a) $q = 0.535$ and (b) $q = 0.53$.

where

$$\theta(j) = j\varphi + \sum_{i=1}^{j} \phi(i), \tag{22}$$

and a random number $\varphi \in [\frac{\pi}{5}, \frac{4\pi}{5}]$. Plotting the trajectories in the (p, s)-plane, the bounded trajectories imply the underlying dynamics is regular (i.e. periodic or quasiperiodic), while Brownian-like (unbounded) trajectories imply the underlying dynamics is chaotic.

For system (9), we set $h = 0.01$ and the initial values $[x_0, y_0, z_0] = [0.1, 0.2, 0.3]$. After abandoning 40 000 data, choosing x-dimensional observable data $n = 100$, its trajectories in the (p, s)-plane are plotted when $q \in [0.5, 0.6]$ and $c = 7$. We find that the trajectories are Brownian-like when $q \geq 0.535$, but the trajectories are bounded when $q \leq 0.53$. Figure 5 shows the trajectories in the (p, s) plane when $q = 0.535$ and $q = 0.53$. So, for $h = 0.01$, it verifies that the lowest order is $3 \times q = 1.605$ when $q = 0.535$ and $c = 7$, and it coincides with that shown in Fig. 3.

Similarly, letting $h = 0.001$, and fixing $c = 5$, the lowest order is 1.35 with $q = 0.45$ as shown in Fig. 6. It is consistent with the results by adopting ADM in [He *et al.*, 2014]. However, in Figs. 1(c)–1(d) and 3, for $h = 0.01$ and $c = 5$, the lowest order is 1.785 with $q = 0.595$. It indicates that the lowest order is affected by iterative step size h. It

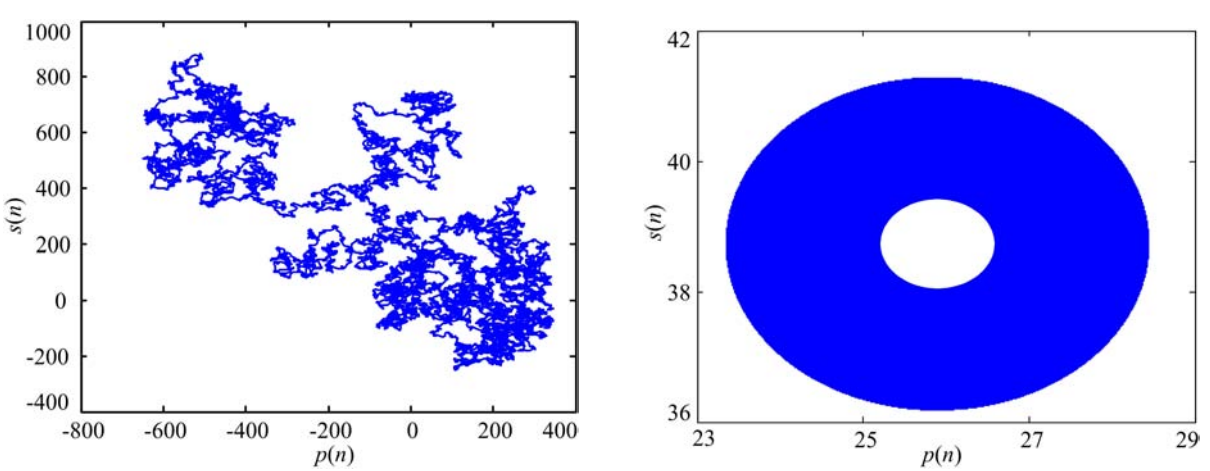

(a) (b)

Fig. 6. For $h = 0.001$ and $c = 5$, the (p, s)-plane for the fractional-order simplified Lorenz system, (a) $q = 0.45$ and (b) $q = 0.44$.

Table 1. Numerical results and performance comparisons with PCM.

Solution Method	Chaos Range		Time Complexity	Space Complexity
	$q = 0.9$	$c = 5$		
ADM	$c \in [-1.1, 7.2]$	$q \in [0.595, 1]$	$O(n)$	$O(1)$
PCM	$c \in [2.6, 7.4]$	$q \in [0.93, 1.07]$	$O(n^2)$	$O(n)$

is an interesting question how step size h affects the dynamics of chaotic systems, which is worthy of further study.

3.4. *Comparisons with the predictor–corrector method*

To compare ADM with PCM, we list chaos range, time complexity and space complexity of the two methods as shown in Table 1. In [Sun *et al.*, 2010a], chaos and bifurcations with $q = 0.9$, c varying and with $c = 5$, q varying were discussed respectively. The bifurcation tendency is similar to our present analysis. However, under the same conditions, the chaos range by adopting ADM is wider than that by adopting PCM (the case of $q > 1$ is not considered in this paper). Some $\mathrm{LE}_{\max}$s were calculated by Wolf algorithm in [Sun *et al.*, 2010a]. But, if one constructs the $\mathrm{LE}_{\max}$ diagram by PCM as in this paper, it could be challenging because of its worse time complexity and space complexity [He *et al.*, 2014].

4. Implementation on DSP

We implement the fractional-order simplified Lorenz system on DSP platform. For hardware design, the block diagram of the working principle is shown in Fig. 7. In the experiments, the Texas Instrument DSP device TMS320F2812 is employed. TMS320F2812 is a 32-bit DSP running at 150 MHz with fixed point operation. Such a high-speed clock rate is considered to be sufficient for our experiments. It can easily interface with a 16-bit dual channels digital-to-analog converter DAC8552 by SPI (serial peripheral interface). Phase portraits of the system are captured randomly by oscilloscope (Tektronix MSO 4102B-L). The platform to implement the chaotic system is shown in Fig. 8.

For software design, based on the discrete iterative Eqs. (11)–(18), the operational procedure is shown in Fig. 9. After initializing DSP, we set the

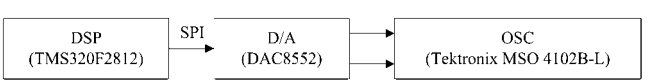

Fig. 7. Simplified block diagram for DSP implementation of a fractional-order chaotic system.

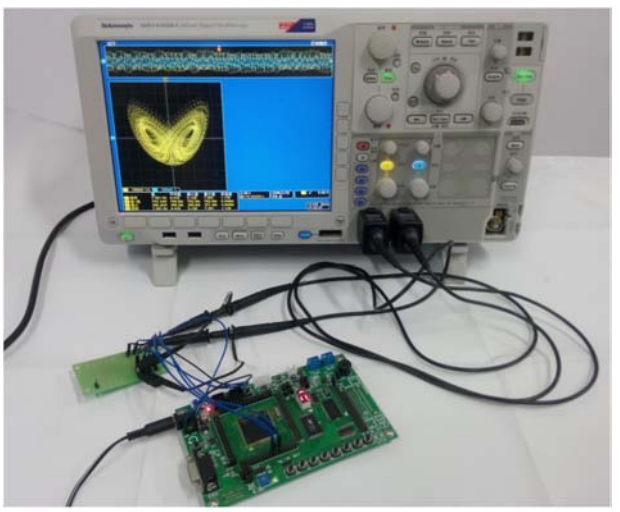

Fig. 8. Platform to implement a fractional-order chaotic system.

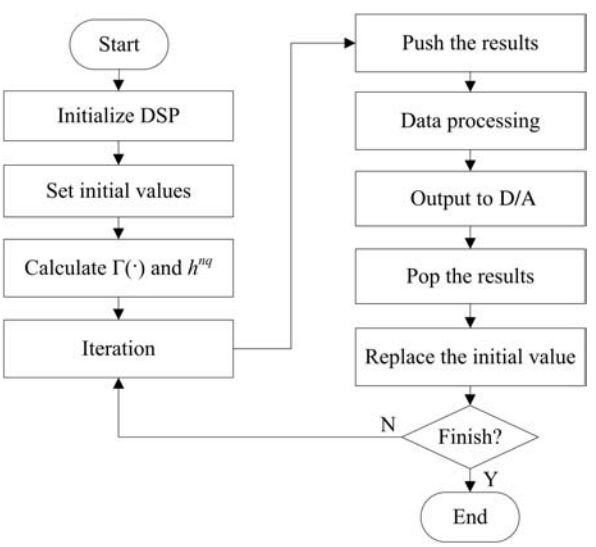

Fig. 9. Flow chart for DSP implementation of a fractional-order chaotic system.

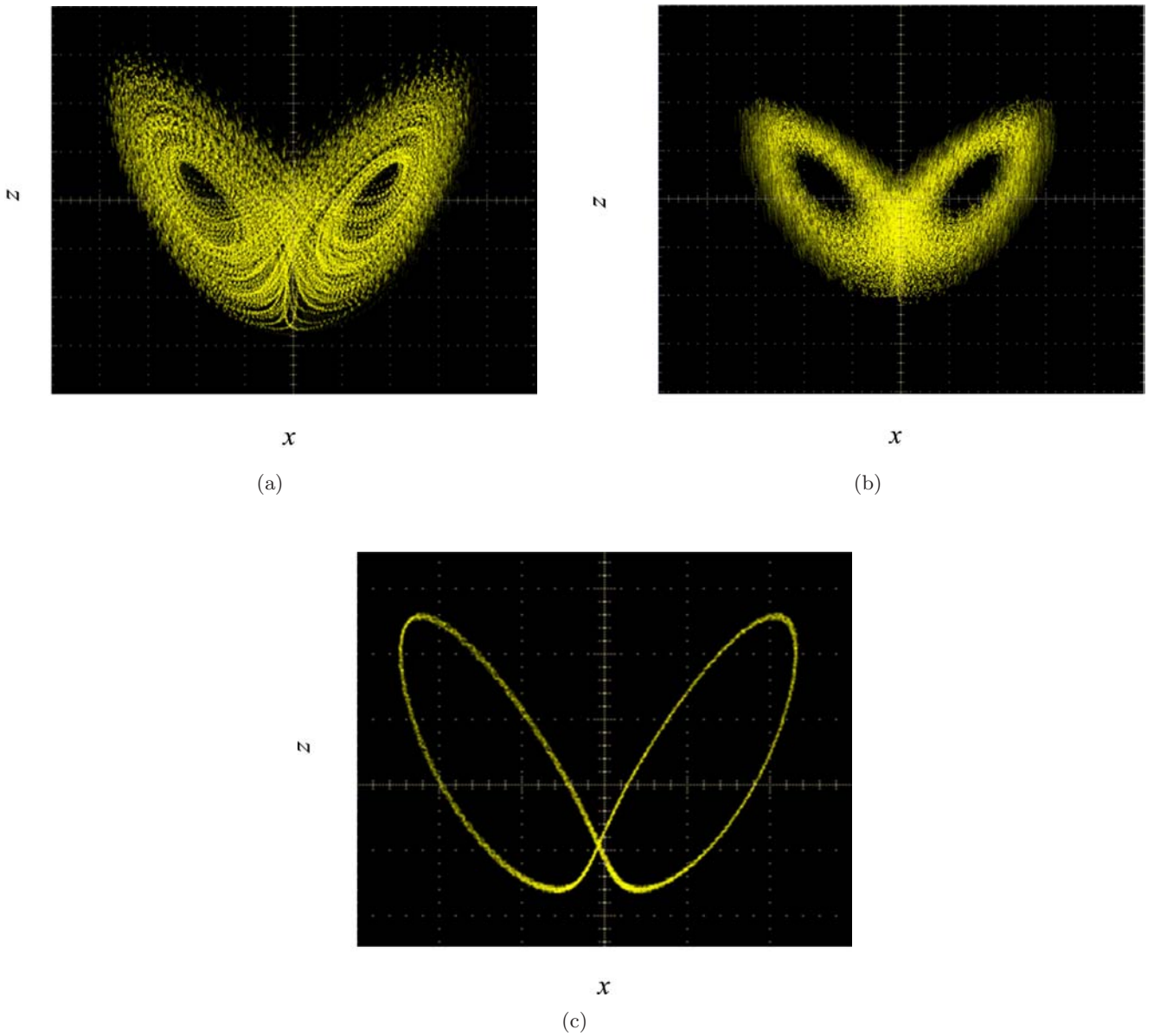

Fig. 10. Phase portraits of attractor for the fractional-order simplified Lorenz system realized on DSP: (a) $q = 0.9, c = 5$; (b) $q = 0.7, c = 3$ and (c) $q = 0.65, c = 7.5$.

initial values, including h, q, $[x_0, y_0, z_0]$, parameters and iteration number. To improve the calculation speed, we calculate all $\Gamma(\cdot)$ and h^{nq} before iterative computation. According to Eqs. (11)–(18), some sequences are negative, and input data of DAC8552 must be integers in $[0, 2^{16} - 1]$. Thus, to display the attractors of the fractional-order chaotic system, the data processing includes three steps. Firstly, a positive integer A is added to all sequences. It makes sure that each data is positive. Secondly, a scaling process is carried out by multiplying a positive integer B. Finally, the above results are rounded up. It is worth mentioning that A and B are different for the sequences with different c and q. In addition, by employing the operation of pushing and popping, the iterative computation is not affected by data processing.

We set $h = 0.01$, initial values $[x_0, y_0, z_0] = [0.1, 0.2, 0.3]$, $A = 15$ and $B = 1400$. Phase portraits of the system are captured by the oscilloscope as shown in Fig. 10. The experimental results qualify the simulation analysis, as shown in Fig. 11. It indicates that the fractional-order simplified Lorenz system is realized successfully on DSP platform.

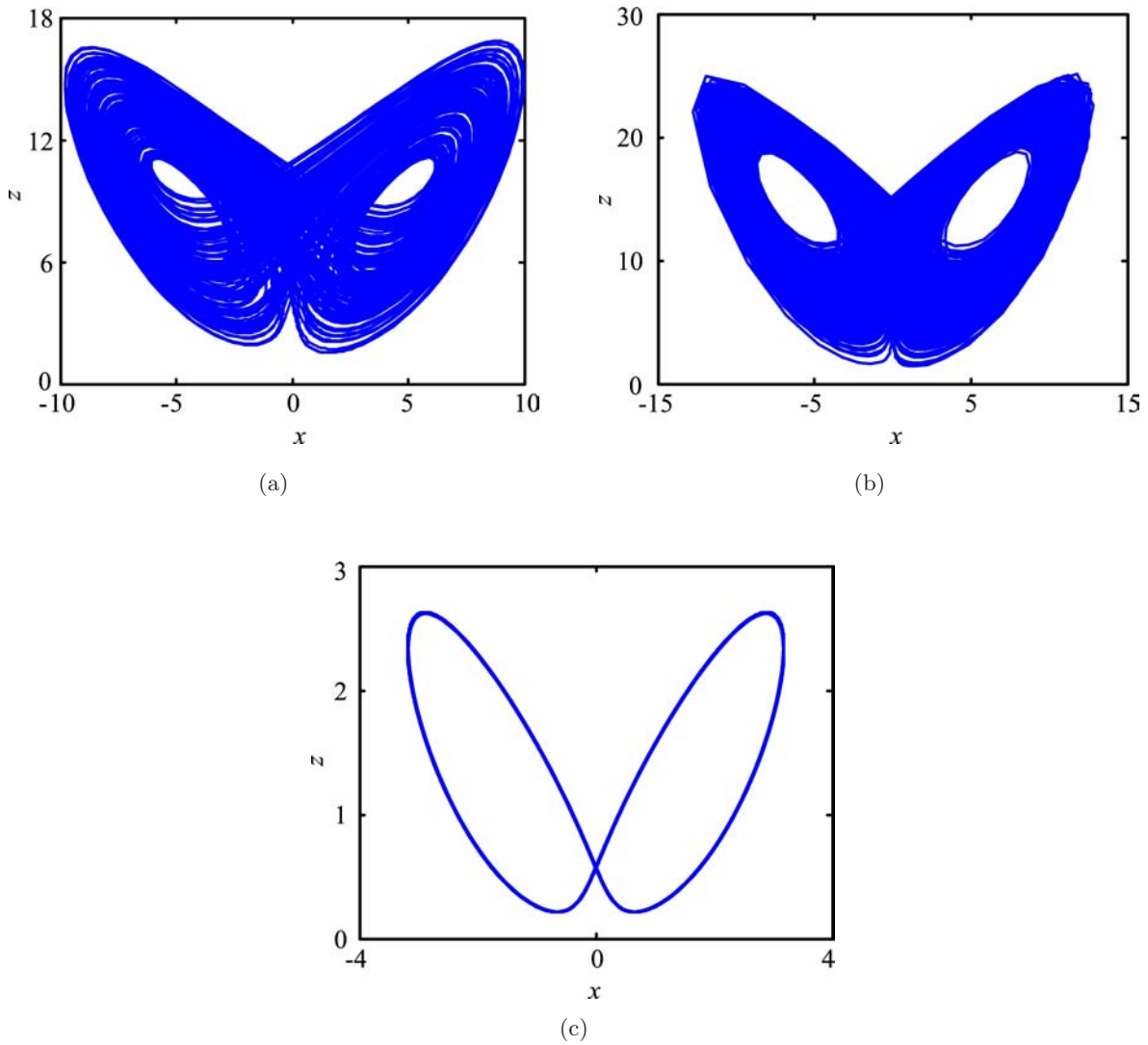

Fig. 11. Phase portraits of attractor for the fractional-order simplified Lorenz system simulated on computer: (a) $q = 0.9, c = 5$; (b) $q = 0.7, c = 3$ and (c) $q = 0.65, c = 7.5$.

In practice, by changing the initial values, parameter c or order q in DSP program, the different states of the fractional-order system are realized. Moreover, as long as the conditions do not change, the results realized on DSP platform are exactly the same. Compared with analog circuit [Jia *et al.*, 2013; Chen *et al.*, 2008], DSP implementations of fractional-order chaotic systems have better flexibility, stability and repeatability, and these advantages will facilitate the application of fractional-order chaotic systems.

5. Conclusions

Based on ADM, the iterative formula of the fractional-order simplified Lorenz system is derived. By employing QR-factorization, the LE spectra calculation algorithm of the fractional-order system is designed. The $\mathrm{LE}_{\max}$ diagram is presented with varying q and c simultaneously. After analyzing the dynamical characteristics of the fractional-order simplified Lorenz system with different fractional derivative orders and parameters, the conclusions are drawn as follows.

(1) When the system is chaotic, for any q, the smaller c is, the larger the $\mathrm{LE}_{\max}$ is, and for parameter c, the smaller q is, the larger the $\mathrm{LE}_{\max}$ is, too. The fractional-order simplified Lorenz system is more complex than its integer-order counterpart.

(2) For ADM and $h = 0.01$, the lowest order of the fractional-order simplified Lorenz system to generate chaos is 1.605. The iteration step

size influences on dynamic characteristics of the fractional-order chaotic system. It is worthy of further study.

(3) The parameters and orders on the boundary should be avoided to be chosen in the practical applications of the fractional-order simplified Lorenz chaotic system.

(4) The fractional-order simplified Lorenz system is implemented on DSP, and it lays the foundation for its extensive applications research in the future.

Acknowledgments

This work was supported by the National Natural Science Foundation of China under Grants 61161006 and 61073187.

References

Abbaoui, K. & Cherruault, Y. [1994] "Convergence of Adomian's method applied to differential equations," *Comput. Math. Appl.* **28**, 103–109.

Adomian, G. [1984] "A new approach to nonlinear partial differential equations," *J. Math. Anal. Appl.* **102**, 420–434.

Bhalekar, S., Daftardar-Gejji, V. & Baleanu, D. [2012] "Transient chaos in fractional Bloch equations," *Comput. Math. Appl.* **64**, 3367–3376.

Cafagna, D. & Grassi, G. [2008] "Bifurcation and chaos in the fractional-order Chen system via a time-domain approach," *Int. J. Bifurcation and Chaos* **18**, 1845–1863.

Cafagna, D. & Grassi, G. [2009] "Hyperchaos in the fractional-order Rössler system with lowest-order," *Int. J. Bifurcation and Chaos* **19**, 339–347.

Cafagna, D. & Grassi, G. [2010] "An effective method for detecting chaos in fractional-order systems," *Int. J. Bifurcation and Chaos* **20**, 669–678.

Caponetto, R. & Fazzino, S. [2013] "An application of Adomian decomposition for analysis of fractional-order chaotic systems," *Int. J. Bifurcation and Chaos* **23**, 1350050-1–7.

Çelik, V. & Demir, Y. [2013] "Chaotic fractional order delayed cellular neural network," in *New Trends in Nanotechnology and Fractional Calculus Applications* (Springer, Netherlands), pp. 313–320.

Chen, X. R., Liu, C. X. & Wang, F. [2008] "Circuit realization of the fractional-order unified chaotic system," *Chin. Phys. B* **17**, 1664–1669.

Daftardar-Gejji, V. & Jafari, H. [2005] "Adomian decomposition: A tool for solving a system of fractional differential equations," *J. Math. Anal. Appl.* **301**, 508–518.

Diethelm, K. [1997] "An algorithm for the numerical solution of differential equations of fractional order," *Electron. Trans. Numer. Anal.* **5**, 1–6.

Gorenflo, R. & Mainardi, F. [1997] *Fractal and Fractional Calculus in Continuum Mechanics* (Springer-Verlag, Wien).

Gottwald, G. A. & Melbourne, I. [2004] "A new test for chaos in deterministic systems," *Proc. Roy. Soc. Lond. Ser. A* **460**, 603–611.

He, S. B., Sun, K. H. & Wang, H. H. [2014] "Solution of the fractional-order chaotic system based on Adomian decomposition algorithm and its complexity analysis," *Acta Phys. Sin.-Ch. Ed.* **63**, 030502.

Hermassi, H., Belazi, A., Rhouma, R. & Belghith, S. M. [2013] "Security analysis of an image encryption algorithm based on a DNA addition combining with chaotic maps," *Multimed. Tools Appl.* **6**, 1–14.

Jia, H. Y., Chen, Z. Q. & Qi, G. Y. [2013] "Topological horseshoe analysis and circuit realization for a fractional-order Lü system," *Nonlin. Dyn.* **74**, 203–212.

Kiani-B, A., Fallahi, K., Pariz, N. & Leung, H. [2009] "A chaotic secure communication scheme using fractional chaotic systems based on an extended fractional Kalman filter," *Commun. Nonlin. Sci. Numer. Simulat.* **14**, 863–879.

Krishna, B. T. [2011] "Studies on fractional order differentiators and integrators: A survey," *Sign. Process.* **91**, 386–426.

Momani, S. & Al-Khaled, K. [2005] "Numerical solutions for systems of fractional differential equations by the decomposition method," *Appl. Math. Comput.* **162**, 1351–1365.

Rhouma, R. & Belghith, S. [2011] "Cryptanalysis of a chaos-based cryptosystem on DSP," *Commun. Nonlin. Sci. Numer. Simulat.* **2**, 876–884.

Salau, T. A. O. & Ajide, O. O. [2012] "Comparative analysis of numerically computed chaos diagrams in Duffing oscillator," *J. Mech. Engin. Autom.* **2**, 53–57.

Shawagfeh, N. T. [2002] "Analytical approximate solutions for nonlinear fractional differential equations," *Appl. Math. Comput.* **131**, 517–529.

Stegemann, C., Albuquerque, H. A. & Rubinger, R. M. [2011] "Lyapunov exponent diagrams of a 4-dimensional Chua system," *Chaos* **21**, 033105.

Sun, H. H., Abdelwahab, A. A. & Onaral, B. [1984] "Linear approximation of transfer function with a pole of fractional power," *IEEE Trans. Automat. Contr.* **29**, 441–444.

Sun, K. H., Wang, X. & Sprott, J. C. [2010a] "Bifurcations and chaos in fractional-order simplified Lorenz system," *Int. J. Bifurcation and Chaos* **20**, 1209–1219.

Sun, K. H., Liu, X. & Zhu, C. X. [2010b] "The 0–1 test algorithm for chaos and its applications," *Chin. Phys. B* **19**, 110510.

Tao, S. & Ue, J. [2014] "Average positive Lyapunov exponent characterization of the parameter plane of harmonically excited pendulum," *Int. J. Eng.* **4**, 26–32.

Tavazoei, M. S. & Haeri, M. [2007] "Unreliability of frequency domain approximation in recognizing chaos in fractional order systems," *IET Sign. Process.* **1**, 171–181.

Tavazoei, M. S. & Haeri, M. [2008] "Limitations of frequency domain approximation for detecting chaos in fractional order systems," *Nonlin. Anal.*: *Math. Appl. Th.* **69**, 1299–1320.

Von Bremen, H. F., Udwadia, F. E. & Proskurowski, W. [1997] "An efficient QR based method for the computation of Lyapunov exponents," *Physica D* **101**, 1–16.

Xavier, J. C. & Rech, P. C. [2010] "Regular and chaotic dynamics of the Lorenz–Stenflo system," *Int. J. Bifurcation and Chaos* **20**, 145–152.

Xin, B. G. & Li, Y. T. [2013] "0–1 test for chaos in a fractional order financial system with investment incentive," *Abstr. Appl. Anal.* **2013**, 876298.